

# Adapting Glass-Ceramic Scintillators from Homeland Security to High-Resolution Medical Imaging

M. Brooke Beckert\*, Jason H. Nadler\* Zhitao Kang\* and Brent K. Wagner\*

\*Georgia Tech Research Institute  
925 Dalney St. Atlanta, GA 30318  
Brooke.Beckert@gtri.gatech.edu

## ABSTRACT

Researchers at GTRI have recently developed a new class of nanocomposite scintillators using glass-ceramic materials. These glass-ceramic scintillators have achieved 18% energy resolution at 662 keV, which is much closer than other composite scintillators to the industry standard of 7% set by NaI(Tl) single crystals. Building on this success, the team began a preliminary study to adapt processes and batch compositions to meet the requirements of medical imaging systems for radiation oncology and dentistry. A 30×40mm specimen containing 30mol% GdF<sub>3</sub> and TbF<sub>3</sub> within an alumino-borosilicate (ABS) host glass was synthesized. Peak emission for the sample was in the green (545nm) regime targeted and the sample showed excellent optical clarity. Additional optical characterization is underway including decay time, light output, modulation transfer function (MTF), and quantum efficiency. Results will inform next steps to increase light output and identify a path to make the glass-ceramics commercially viable by increasing batch size.

**Keywords:** glass-ceramics, scintillators, medical imaging, radiation detection

## 1 INTRODUCTION

Inorganic scintillators convert energy from incident high energy ionizing radiation (shown schematically in Figure 1) into thousands of lower energy photons via electron transitions between the valence ( $E_1$ ) and conduction bands ( $E_2$ ) of a host crystal (such as Gd<sub>2</sub>O<sub>3</sub>) doped with a rare-earth activator (such as Ce<sup>3+</sup> or Tb<sup>3+</sup>). The dashed arrows in Figure 1 represent non-radiative transitions in which no photons are produced, whereas the solid arrows indicate transitions in which electron-hole pairs are created or recombine by releasing a photon. The energy separation between the excited ( $E'_2$ ) and ground ( $E'_1$ ) states of the activator dopant dictate the energy, and thus the wavelength, of the scintillation photons produced when the electron-hole pairs recombine<sup>1</sup>. This excitation and recombination scheme will, ideally, occur many thousands of times per millisecond.

By changing the activator dopant, the wavelength of scintillation photons can be tailored to match the spectral sensitivity of the collection optics used to convert the photons into an electrical signal<sup>2</sup>. For example, Ce<sup>3+</sup> centers are used to produce 350nm photons collected by photomultiplier

tubes (PMTs) for homeland security, while Tb<sup>3+</sup> activators are used to produce 540nm photons collected by amorphous silicon photodiodes for medical imaging systems<sup>3,4</sup>.

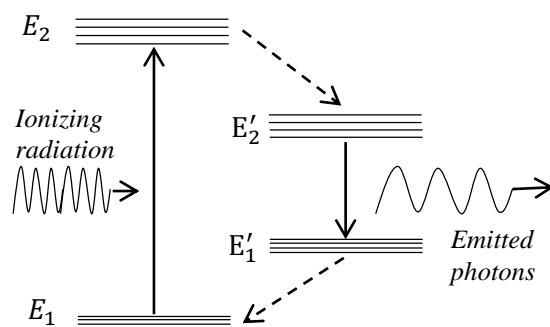


Figure 1: Schematic of the scintillation process; Incident high-energy radiation (1) excites electrons from the valence band of the host crystal ( $E_1$ ) to the conduction band ( $E_2$ ). The electron-hole pairs are non-radiatively transferred (2) to the dopant cation and recombine from  $E'_2$  to  $E'_1$  by emitting a lower energy photon (3).

In homeland security applications, the electrical signal produced by the PMT is analyzed to create an energy spectrum by which the source radioisotope emitting the ionizing radiation can be identified<sup>5</sup>. In medical imaging systems, the electrical signal creates a digital image with high density contrast which allows clinicians to identify tumors or other problem tissues. Both applications rely on scintillators that produce a high light output, which is defined as the number of photons emitted per unit energy of ionizing radiation absorbed by the scintillator.

To produce a high light output, the scintillator must have an ordered, periodic lattice structure. This reduces the statistical variance in electron-hole recombination modes, and ensures that a large fraction of the relaxation processes are radiative<sup>5</sup>. If the lattice periodicity is disturbed due to microstructural defects or breakdown in long-range order, new recombination or relaxation modes are introduced, which can either produce photons outside of the desired wavelength range or allow electrons to relax via non-radiative lattice vibrations (phonons)<sup>1</sup>. Good optical clarity of the scintillator is also needed to minimize the number of emitted photons that are scattered or re-absorbed<sup>6</sup>. Thus, the scintillator must be highly transparent to the wavelength of emitted photons and have minimal defects such as grain boundaries or compositional impurities that scatter photons.

Since the mid-20<sup>th</sup> century, these criteria have been met by growing large volume (>5,000cm<sup>3</sup>) single crystals of thallium-doped sodium iodide (NaI(Tl)) or cesium iodide (CsI(Tl)). These crystals are grown by melting very high purity (>99.99%) precursor materials under an inert atmosphere, and then introducing a “seed” crystal to provide a template for growth. The seed crystal is pulled slowly upward out of the melt at a rate of approximately 2mm per hour to allow additional liquid to solidify onto the pattern and eventually yield a large volume single crystal from which smaller crystals can be cut <sup>7</sup>. The inert atmosphere is required because the alkali halide salts are very hygroscopic and will degrade in a matter of hours if exposed to environmental humidity. The high purity raw materials required, combined with complex synthesis and post-processing significantly increases the cost of single crystal scintillators.

To address the need for high light yield scintillators at a more competitive price point, investigators at the Georgia Tech Research Institute (GTRI) developed new composite scintillators using glass-ceramic nanocomposite materials. Glass-ceramics are composites in which discrete crystalline phases have been selectively precipitated from an amorphous host glass matrix during a heat treatment step known as ceramization <sup>8</sup>. In the case of nanocomposite scintillators, the size of the crystallites is kept below 50nm to prevent scattering of emitted light. Furthermore, rare-earth crystal and dopant compositions already in use can be synthesized using the glass-ceramics approach, which ensures that the new scintillators can be integrated into existing radiation detection and medical imaging hardware.

Some of the most attractive advantages of this approach are that batches can be scaled to tailor scintillator size to suit the hardware of the system, the hygroscopic crystals are isolated from environmental humidity and so secondary encapsulation is not required, and more complex geometries are feasible by casting the glass melt into the desired shape. The authors have shown the advantages of this approach in homeland and border security screening applications <sup>9-12</sup>, and now are adapting these concepts to suit the medical imaging space. The following sections present an overview of the standard synthesis process and specific modifications needed to ensure the glass-ceramics meet the requirements for integration into medical imaging systems.

## 2 SCINTILLATORS FOR HOMELAND SECURITY

The GTRI team originally developed the glass-ceramic scintillators as part of an effort jointly funded by the National Science Foundation and Department of Homeland Security, and thus batch composition and processing methods were designed to meet performance benchmarks for isotope detection and identification. The most critical benchmarks were the energy resolution, which is reported as the full-width at half maximum of the 662 keV photopeak produced in response to Cs-137 gamma-rays <sup>5</sup>, and the peak emission

wavelength, which should be from 350-450nm to match the spectral sensitivity of PMTs. Secondary criteria included the range of radiation energies and types of source isotope for which the scintillators could produce an energy spectrum. The stainless steel casing on NaI(Tl) single crystals has typically limited their application to gamma-ray detection because the casing prevents other types of radiation, such as alpha or beta particles, from reaching the crystal <sup>13</sup>. However, glass-ceramic scintillators do not require encapsulation, and so sensitivity to alpha and beta particles as well as neutrons was preserved. This means that security personnel can now detect and identify multiple types of radiation sources with a single piece of hardware where previously they needed an array of detection systems to achieve the same performance.

### 2.1 Materials Selection & Synthesis

The investigation began by selecting promising candidate materials for the oxide host glass and the rare-earth halide scintillating crystals. The oxide host glass was selected based on the free volume available in the glass network, melting temperature, and ease of glass formation. A large network free volume is needed to create high solubility for the rare-earth halide solute while maintaining transparency. A relatively low melting temperature (<1400°C) helps reduce the processing temperatures required to homogenize the glass melt, which in turn helps to minimize volatilization of the lower melting temperature (800°C) rare-earth halides during heating. Finally, ease of glass formation is needed to prevent devitrification (crystallization) of the glass melt during quenching. Spontaneous crystallization during cooling does not yield the nano-scale crystallites required for high optical clarity, and crystallization of the host glass matrix causes emitted photons to be absorbed. Based on these criteria, an aluminoborosilicate (ABS) base glass was selected <sup>14</sup>. The alumina and silica content forms a network of oxygen-linked tetrahedra, creating a large network free volume and high solubility for rare-earth halides. The addition of boron and sodium oxide provides an acceptable depression of the melting temperature while maintaining ease of glass formation.

Rare-earth halides for the scintillating crystallites were selected based on density, peak emission, and theoretical light output. A high density was needed to ensure the high energy incident radiation is fully absorbed within the scintillator volume, thus maximizing light output. Emission wavelength, as stated previously, must match the peak spectral sensitivity of the collection optics, which is 350nm for homeland security applications. Based on these criteria, cerium-doped gadolinium bromide was selected. These high density lanthanide series elements exhibit efficient energy transfer between the two cations, and peak emission (for Ce<sup>3+</sup>) at 350nm <sup>15</sup>.

Once the appropriate materials were selected, the glass-ceramic scintillators were synthesized by mixing precursor powders of the ABS host glass with varying concentrations of GdBr<sub>3</sub> and CeBr<sub>3</sub>. The mixture was loaded into an alumina

crucible and covered with an alumina plate. A reducing purge gas mixture was applied to the crucible to ensure the  $Ce^{3+}$  activator dopants remain in the trivalent valence state needed to produce blue emission. The mixture was heated to 1400°C and allowed to dwell for 2-4 hours to homogenize the melt. The crucible was removed from the furnace and the melt cast into a pre-heated graphite mold of the desired volume and geometry, and then annealed to remove thermal stresses.

Differential thermal analysis (DTA) scans were acquired for small (150mg) powder samples taken from each glass batch composition to determine the temperature required for the ceramization step. The ceramization temperature varied from 700°C to 850°C depending on the composition and concentration of rare-earth compounds used. Once the ceramization temperature was determined, glass samples were heated to the specified temperature and held for 2-48 hours to evaluate the effect of dwell time on the size of precipitated crystallites. Glass-ceramic parts were then polished for optical characterization.

This synthesis procedure was used to produce specimens sizes from 15cm<sup>3</sup> to 50cm<sup>3</sup> with up to 30mol% scintillating compounds incorporated while maintaining scintillator transparency. These glass-ceramic scintillators exhibited better detection and identification performance than any other composite scintillator developed during the multi-year program. The glass-ceramics shown in Figure 2 yielded energy spectra for alpha and beta particles, gamma-rays, and neutrons, and achieved a maximum energy resolution of 18% at 662 keV, as shown in Figure 3. The team has continued to refine processing techniques and batch compositions to further increase light yield.



Figure 2: Cerium-doped glass-ceramic scintillators under ambient (left) and UV exposure (right)

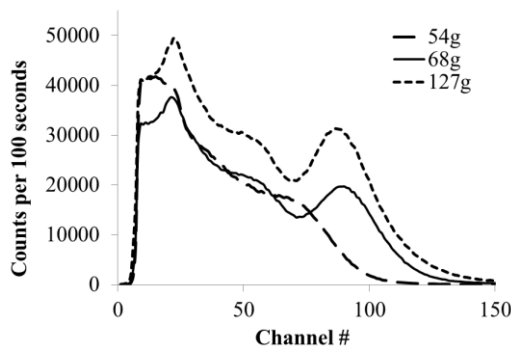


Figure 3: Energy spectra for Cs-137 gamma-rays from glass-ceramic scintillators of varying size

### 3 ADAPTING SCINTILLATORS FOR MEDICAL IMAGING

The authors have now begun to modify the composition and processing of glass-ceramic scintillators to suit the needs of diagnostic medical imaging and radiation oncology. These application areas typically employ gadolinium oxysulfide phosphors doped with terbium (GOS)<sup>16</sup> or thallium-doped cesium iodide single crystals<sup>17</sup> or crystal arrays, depending on the image resolution needed. For example, the high resolution images produced with 60-80keV X-rays and GOS panels are needed when clinicians must precisely locate the tumor with respect to healthy tissue and organs, and then position the patient on the treatment couch so that dosage to non-cancerous tissues during radiation therapy is minimized. Because 60-80 keV X-rays are used to acquire the images, these imaging panels are referred to as “kV” panels. The fabrication process for these panels is fairly straightforward because the phosphor powders are not sensitive to environmental moisture and are micron-sized, and so do not require specialized nano-scale synthesis routes. Thus, kV panels are very economical and cost around \$200 per 30×40cm panel.

When image quality requirements are less stringent, but dosimetry and evaluation of the treatment beam are of interest, clinicians utilize an imaging panel comprised of a single crystal or polycrystalline array of cesium-iodide (CsI). The high density crystals are able to more fully absorb the higher energy radiation (10 MeV) used for radiation therapy, and allow clinicians to verify that the accelerator is operating within acceptable limits. These CsI crystals are referred to as “MV” panels due to the higher energy X-rays used. In contrast to the GOS phosphors, CsI crystals are extremely sensitive to environmental moisture and will degrade in a matter of hours if not hermetically sealed. In panels where a single crystal is required, high purity precursor materials must be melted in an inert atmosphere and grown using one of the standard single crystal growth techniques, which typically achieve a growth rate of approximately 1-2 mm per hour. Additional machining and post-processing are then needed to achieve the dimensions specified for the end application, all of which must take place in inert atmospheres. Thus, CsI crystals are significantly more expensive than their GOS screen counterparts, costing nearly \$25,000 per 40×30cm panel.

Glass-ceramic scintillators are promising alternatives to both the GOS screens and CsI crystals. Higher transparency and light output compared to GOS screens may allow lower X-ray energies to be used to produce images of comparable resolution. This would lower the dosage to the patient during imaging, which is especially attractive in pediatrics. In addition, the melt synthesis approach produces large volume scintillators much more quickly than single crystal growth, and forming the nanoscale scintillating crystals within a glass matrix precludes the need for secondary encapsulation to prevent degradation. Thus, glass-ceramic scintillators offer considerable cost savings relative to CsI arrays.

The first step in adapting glass-ceramic scintillators for use in medical imaging systems was to shift the emission peak from 350nm (blue) to 540nm (green) to match the spectral sensitivity of the amorphous silicon photodiode panels used in most imagers. The simplest approach was to use a rare-earth composition the closely matched the GOS screens currently used. Thus, gadolinium was selected for the host crystal and  $Tb^{3+}$  for the activator dopant. Gadolinium fluoride, which should have a higher light yield, was used in place of gadolinium oxysulfide. The ABS host glass composition was unchanged from that used in the blue-emitting scintillators.

Small scale (50g) proof-of-concept batches were prepared using the same processing methods described in the preceding sections, with  $GdF_3$  used in place of the  $GdBr_3$  and  $TbF_3$  used in place of  $CeBr_3$ . The glass melt was cast into a  $40 \times 50 \times 5$ mm stainless steel mold and squeezed to form a rectangular coupon, as shown in Figure 4. The coupon was annealed, and then diced and polished for optical characterization, which is ongoing. Preliminary data show that peak emission occurs at 545nm. Additional data will be collected for decay time, light output, modulation transfer function (MTF), and transmittance.



Figure 4: Glass-ceramic specimen containing 30mol%  $GdF_3(Tb)$  under UV (left) and ambient light (right)

As seen in the above image, the glass-ceramic coupon was highly transparent with very few trapped bubbles and no visible secondary phases. Optical characterization data will inform next steps, but based on feedback from industry partners, the team anticipates that the next priority will be to increase density to maximize absorption cross section by maximizing the concentration of rare-earth compounds in the batch. Both of these modifications will increase light output and make the glass-ceramic scintillators a viable alternative to existing GOS screens and CsI crystals. In parallel, the team will determine process modifications needed to ensure melt homogeneity and removal of bubbles as batch size is scaled to near commercial levels. A custom glass batching furnace equipped with a mechanical stirring mechanism has recently been installed at GTRI to increase batch scale to over 250g while preserving optical clarity.

#### 4 SUMMARY

GTRI researchers have developed novel glass-ceramic nanocomposite scintillators for use in homeland security and border screening applications. The glass-ceramic specimens produced have shown considerable promise as alternatives to single crystal scintillators. The glass-ceramics approach is

advantageous because it eliminates agglomeration of nanoparticles and encapsulates hygroscopic rare-earth halide nanocrystals in a stable oxide glass, protecting them from environmental humidity. Preliminary work is underway to adapt the processing methods developed and compositions optimized to suit the requirements of medical imaging applications. Results from optical characterization will quantify performance relative to GOS screens and CsI crystals, and data is expected within the coming months.

#### REFERENCES

- (1) Rodnyi, P. *Physical Processes in Inorganic Scintillators*; CRC Press: Boca Raton, FL, 1997.
- (2) Yoshioka, T.; Ogawa, M. In *Phosphor Handbook*; Taylor & Francis Group, LLC, 2006.
- (3) Nakazawa, E. In *Phosphor Handbook*; Taylor & Francis Group, LLC, 2006.
- (4) Miura, N. In *Phosphor Handbook*; Taylor & Francis Group, LLC, 2006; Vol. 54.
- (5) Knoll, G. F. *Radiation Detection and Measurement*, 4th ed.; John Wiley & Sons, Inc.: Hoboken, NJ, 2010.
- (6) Price, W. J. *Nuclear Radiation Detection*, 1st ed.; Zinn, W. H., Luntz, J. D., Eds.; McGraw-Hill Book Company, Inc.: New York, 1958.
- (7) Higgins, W. M.; Churilov, A.; van Loef, E. V.; Glodo, J.; Squillante, M.; Shah, K. S. *J. Cryst. Growth* **2008**, *310* (7-9), 2085–2089.
- (8) Strnad, Z. *Glass-Ceramic Materials*, 1st ed.; Elsevier: New York, 1986.
- (9) Barta, M. B.; Nadler, J. H.; Kang, Z.; Wagner, B. K.; Rosson, R.; Kahn, B. *Opt. Mater. (Amst)*. **2013**, *36* (2), 287–293.
- (10) Barta, M. B.; Nadler, J. H.; Kang, Z.; Wagner, B. K.; Rosson, R.; Cai, Y.; Sandhage, K. H.; Kahn, B. *Appl. Opt.* **2014**, *53* (16), D21–D28.
- (11) Kang, Z.; Rosson, R.; Barta, M. B.; Han, C.; Nadler, J. H.; Dorn, M.; Wagner, B.; Kahn, B. *Radiat. Meas.* **2013**, *48*, 7–11.
- (12) Han, C.; Barta, M. B.; Dorn, M.; Nadler, J. H.; Rosson, R.; Wagner, B.; Kahn, B.; Kang, Z. *Proc. SPIE* **2011**, *8142*, 81420R.
- (13) Milbrath, B. D.; Peurrung, A. J.; Bliss, M.; Weber, W. J. *J. Mater. Res.* **2008**, *23* (20), 2561–2581.
- (14) Li, L.; Li, H.; Maoxu, Q.; Strachan, D. M. *J. Non. Cryst. Solids* **2001**, *283* (1-3), 237–245.
- (15) Van Loef, E. V. *Opt. Commun.* **2001**, *189* (4-6), 297–304.
- (16) Mathers, J. E.; Yale, R. L. Terbium-activated gadolinium oxysulfide X-ray phosphor. 4,507,560, 1985.
- (17) Svenonius, O.; Sahlholm, A.; Wiklund, P.; Linnros, J. *Nucl. Instruments Methods Phys. Res. Sect. A Accel. Spectrometers, Detect. Assoc. Equip.* **2009**, *607* (1), 138–140.